Article:
Vanhinsbergh, C., Hook, E.C., Oxby, N. et al. (1 more author) (2023) Optimization of orthogonal separations for the analysis of oligonucleotides using 2D-LC. Journal of Chromatography B, 1227. 123812. ISSN 1570-0232

https://doi.org/10.1016/j.jchromb.2023.123812

Journal of Chromatography B 1227 (2023) 123812

Contents lists available at ScienceDirect

Journal of Chromatography B

journal homepage: www.elsevier.com/locate/jchromb

Optimization of orthogonal separations for the analysis of oligonucleotides using 2D-LC

Christina Vanhinsbergh [a], Elliot C. Hook [b], Nicola Oxby [b], Mark J. Dickman [a,*]

[a] Department of Chemical and Biological Engineering, Mappin Street, University of Sheffield, S1 3JD, UK
[b] GlaxoSmithKline, GSK Medicines Research Centre, Gunnels Wood Road, Stevenage, Herts SG1 2NY, UK

ARTICLE INFO

Keywords:
Oligonucleotides
HPLC
2D HPLC
Ion pair reversed phase HPLC
Anion exchange HPLC

ABSTRACT

Oligonucleotides are commonly analysed using one dimensional chromatography (1D-LC) to resolve and characterise manufacturing impurities, structural isomers and (in respect to emerging oligonucleotide therapeutics) drug substance and drug product. Due to low selectivity and co-elution of closely related oligonucleotides using 1D-LC, analyte resolution is challenged. This leads to the requirement for improved analytical methods. Multi-dimensional chromatography has demonstrated utility in a range of applications as it increases peak capacity using orthogonal separations, however there are limited studies demonstrating the 2D-LC analysis of closely related oligonucleotides. In this study we optimised OGN size and sequence based separations using a variety of 1D-LC methods and coupled these orthogonal modes of chromatography within a 2D-LC workflow. Theoretical 2D-LC workflows were evaluated for optimal orthogonality using the minimum convex hull metric. The most orthogonal workflow identified in this study was ion-pair reversed phase using tributylammonium acetate (IP-RP-TBuAA) coupled with strong anion exchange in conjunction with sodium perchlorate (SAX-$NaClO_4$) at high mobile phase pH. We developed a heart-cut (IP-RP-TBuAA)-(SAX-$NaClO_4$) 2D-LC method for analysis of closely related size and sequence variant OGNs and OGN manufacturing impurities. The 2D-LC method resulted in an increased orthogonality and a reduction in co-elution (or close elution). Application of a UV based reference mapping strategy in conjunction with the 2D-LC method demonstrated a reduction in analytical complexity by reducing the reliance on mass based detection methods.

1. Introduction.

Oligonucleotides (OGNs) are used in a wide range of biochemical applications and OGN therapeutics are emerging as an important class of pharmaceuticals that control gene expression, splicing or translation events and bind to target ligands [1-6]. High performance liquid chromatography (HPLC) is widely used for the analysis of OGNs including OGN therapeutics and their related manufacturing impurities. The separation and characterisation of complex mixtures of OGNs and OGN impurities poses a significant analytical challenge, as complex samples or OGN manufacturing impurities are very closely related structures that are difficult to resolve using chromatography [7,8]. Synthetic OGNs are commonly manufactured by solid phase synthesis [9], resulting in the creation of failure sequences such as shortmers, longmers or isomers during manufacture [10-13]. These OGN impurities may differ from the target OGN by as little as one nucleotide, hold alternative structural conformations and their levels are important quality attributes to report as contributions to regulated OGN therapeutic safety and toxicology studies [14,15].

The analysis of OGNs using 1D-LC has been developed using a range of modes, such as anion exchange, ion-pair reversed-phase, hydrophilic interaction and size exclusion chromatography [16-27]. Utilisation of ion-pair reversed-phase (IP-RP) HPLC enables OGN separations based upon both size (in nucleotides) and base sequence [27,28]. We have previously used IP-RP HPLC for the analysis of OGNs in a wide variety of applications and provided further insight into the mechanisms of OGN separations [29-33]. The dominance of separation based upon size or sequence can be manipulated by altering the hydrophobicity of the alkyl amine ion-pair reagent (IPR) or addition of a fluorinated acidic alcohol, such as hexafluoroisopropanol (HFIP), to the IP-RP mobile phase [34,35]. Increasing the IPR hydrophobicity facilitates stronger interactions between the IPR and stationary phase, blocking secondary interactions between OGN nucleobases and the stationary phase and increasing dynamic ion exchange processes [27]. HFIP also increases

* Corresponding author.
E-mail address: m.dickman@sheffield.ac.uk (M.J. Dickman).

https://doi.org/10.1016/j.jchromb.2023.123812
Received 28 April 2023; Received in revised form 28 June 2023; Accepted 30 June 2023
Available online 1 July 2023

dynamic ion exchange by increasing IPR adsorption towards the stationary phase- thus increasing the concentration of IPR upon the stationary phase surface [35,36]. Increased dynamic ion exchange processes and inhibition of secondary interactions between OGN bases and the stationary phase result in OGN size dominant separations. OGN separation mechanisms can also be manipulated by altering chromatographic conditions, such as temperature and mobile phase velocity to effect mass transfer processes [28]. Strong anion exchange (SAX) HPLC also demonstrates both size and sequence dependent OGN separation mechanisms. The OGN phosphodiester bonds each contribute to the net anionic charge in a size dependent manner. Increased SAX mobile phase pH further ionises tautomeric guanine and thymine nucleobases in addition to the OGN phosphate backbone [20]. Increased ionisation of OGN nucleobases results in increased base sequence dominant separation mechanisms under SAX chromatographic conditions.

1D-LC using both IP-RP and SAX approaches can resolve OGNs up to 59 nucleotides in size by a single nucleotide [16,37]. However, 1D-LC remains challenged by close and co-elution of OGNs of similar size, base composition and sequence [38]. This is further complicated by the addition of chemical modifications to OGNs, which increases the complexity of their molecular chemistry [39]. These challenges inhibit the characterisation of complex OGN mixtures or analysis of manufacturing batches containing impurity OGNs at low concentration to the target OGN [40,41]. Improved chromatographic separations use multidimensional orthogonal approaches to increase peak capacity and resolution. Two-dimensional chromatography (2D-LC) resolves analytes using orthogonal separations and has demonstrated utility in improving analysis of a range of molecules, including peptides, polymers and pharmaceuticals [42-46]. There are limited studies demonstrating 2D-LC methods for the analysis of OGNs, however previous studies have demonstrated improved resolution of homopolymeric OGNs using comprehensive (hydrophilic interaction or HILIC) x(IP-RP) 2D-LC [47] and offline comprehensive 2D-LC that interfaced either IP-RP or SAX HPLC with capillary gel electrophoresis [48]. (IP-RP)-(IP-RP) 2D-LC has also been used to resolve fluorophore dual labelled OGNs from modification failures prior to analysis of length variants [49]. Roussis et al applied 2D-LC-MS analysis to a range of OGNs [50]. 2D-LC methods implementing RP, SAX and IP-RP facilitated the resolution of protected and deprotected OGN impurities, phosphorothioated OGN synthesis impurities from the target OGN product. Most recently, heart-cut (SAX/IP-RP)-(HILIC) 2D-LC methods were developed for the analysis of antisense OGN impurities [51].

In this study, initial work focussed on the optimisation of 1D-LC separations for size or sequence dominant separations- based upon OGN size in nucleotides or OGN base sequence respectively. The orthogonality of theoretical 2D-LC workflows was analysed using the minimum convex hull metric of orthogonality assessment [52]. The 2D-LC workflow of (IP-RP-TBuAA)-(SAX) was further optimised and developed for the analysis of closely related OGNs. A range of size and sequence variant OGNs and a representative OGN manufacturing sample (containing typical manufacturing impurities) were analysed using heart-cut (IP-RP)-(SAX) 2D-LC. Typically OGNs and their associated manufacturing impurities are characterised using HPLC coupled with mass spectrometry (LC-MS) to identify analytes using their mass to charge ratios. LC-MS based approaches require a high level of technical expertise to analyse data in addition to high equipment costs. The 2D-LC method, developed in this work was optimised to characterise OGNs using UV spectrophotometry in conjunction with OGN reference mapping to reduce the complexity of the analytical method. However, mass spectrometry was utilised to establish the reference mapping strategy during method development. The 2D-LC method demonstrated a reduction in co-elution of OGNs and an increase in peak capacity in all sample sets. The reference mapping strategy successfully characterised OGNs in each sample using UV detection.

2. Methods

2.1. Chemicals and reagents

Acetonitrile (MeCN, HPLC grade Fisher Scientific, UK), Triethylammonium acetate buffer (1 M, pH 7, TEAA, Sigma Aldrich, UK), Tributylamine 99% (TBA, Acros Organics, UK), Glacial Acetic Acid (HPLC grade, J T Baker, UK), Sodium perchlorate monohydrate ($NaClO_4$ 97% Alpha Aesar, UK), Tris(hydroxymethyl)aminomethane (99.9%, Tris, Sigma Aldrich, UK), 1,1,1,3,3,3-Hexafluoro-2-propanol (99%, HFIP, Sigma Aldrich, UK), Tetrasodium ethylenediaminetetraacetate hydrate (99%, Na_4 EDTA, Sigma Aldrich, UK), Water (HPLC grade, Fisher Scientific, UK), Sodium hydroxide (98%, NaOH, Sigma Aldrich, UK). All oligonucleotides were synthesised by Eurofins Scientific (UK) (see Table 1).

2.2. HPLC analysis

All mobile phases were prepared with HPLC grade solvents (Fisher Scientific, UK). SAX mobile phases were prepared to correct pH using a pH meter and NaOH. A stock solution of 100 mM TBuAA was prepared by adding 6 ml tributylamine to 225 ml MeCN and 1.5 ml glacial acetic acid under inert gas and adding water to 250 ml volume. This stock was used when preparing IP-RP (TBuAA) mobile phases at lower concentration. The stock was stored under inert gas to prevent oxidation of the IPR.

OGNs were analysed using a Thermo Scientific (Dionex) U3000 RSLC (U)HPLC. *Configuration 1* was used for IP-RP (TBuAA), IP-RP (TEAA) and SAX 1D-LC and all 2D-LC methods. *Configuration 2* was used for HFIP modified IP-RP (TEAA:HFIP) 1D-LC. IP-RP analysis was performed using DNAPac RP columns (2.1 mm ID × 100 mm) and SAX HPLC analysis was performed using a DNAPac PA200 Rs column (4.6 mm ID × 150 mm). Chromatograms were recorded using a UV–Vis detector at 260 nm wavelength. Viper MP35N biocompatible tubing was used at 0.1 mm ID for IP-RP HPLC analysis (at 0.2 ml min^{-11} mobile phase velocity) and 0.18 mm ID for SAX HPLC analysis (at 0.8 ml min^{-1}).

Configuration 1: Thermo Scientific (Dionex) U3000 (U)HPLC with the following modules: SRD-3600 degasser, DGP-3600RS dual ternary pump system, WPS-3000TFC autosampler with fractionation valve, TCC-3000SD fan assisted column oven with 2* multi switch valves and a VWD-3400RS UV–VIS multi wavelength detector.

Configuration 2: Thermo Scientific (Dionex) U3000 (U)HPLC with the following modules: LPG-3400RS quaternary pump system, WPS-3000TBFC autosampler with fractionation valve, TCC-3000RS fan assisted column oven and a VWD-3400RS UV–VIS multi wavelength detector.

2.3. HPLC mobile phases

2.3.1. HFIP modified IP-RP (TEAA:HFIP) HPLC

Mobile phase A: 100 mM TEAA, 40 mM HFIP, 0.1 mM Na_4 EDTA. HFIP modified IP-RP (TEAA:HFIP). Mobile phase B: 100 mM TEAA, 40 mM HFIP, 0.1 mM Na_4 EDTA, 25% $^{v}/_{v}$ MeCN.

2.3.2. IP-RP (TBuAA) HPLC

Mobile phase C: 5 mM TBuAA, 0.1 μM Na_4 EDTA, 10% $^{v}/_{v}$ MeCN. IP-RP (TBuAA) Mobile phase D: 5 mM TBuAA, 0.1 μM Na_4 EDTA, 80% $^{v}/_{v}$ MeCN.

2.3.3. IP-RP (TEAA) HPLC

Mobile phase E: 100 mM TEAA, 0.1 mM Na_4 EDTA. IP-RP (TEAA) Mobile phase F: 100 mM TEAA, 0.1 mM Na_4 EDTA, 25% $^{v}/_{v}$ MeCN.

2.3.4. SAX HPLC

Mobile phase G: 20 mM Tris pH 11.5, 20% $^{v}/_{v}$ MeCN. SAX Mobile phase H: 20 mM Tris, 400 mM $NaClO_4$ pH 11.5, 20% $^{v}/_{v}$ MeCN.

Table 1
Model DNA OGNs used for the evaluation of size and sequence dependent separations and development of 2D-LC analytical methods. OGNs are described by size in nucleotides (nt), base sequence and monoisotopic mass in daltons (Da). Size and sequence variant OGNs in test set 1 are highlighted in blue and OGNs in test set 2 are highlighted in green. A '*' indicated a phosphorothioate bond.

OGN	OGN Description	Sequence	Length (nt)	Mass (Da)
Size & Sequence isomers	19-mer i	CTA GTT ATT GCT CAG CGG T	19	5807.0
	19-mer ii	CGC CAT CCA CGC TGT TTT G	19	5728.0
	19-mer iii	ATT AGG ACA AGG CTG GTG G	19	5930.0
	19-mer iv	AGA GTT TGA TCA TGG CTC A	19	5840.0
	20-mer i	GGG ATG TTT AAT ACC ACT AC	20	6113.1
	20-mer ii	CCC TCA TAG TTA GCG TAA CG	20	6074.0
	20-mer iii	TTG CTG TTG CAC AGT GAT TC	20	6111.0
	20-mer iv	GGC AGC AGC CAC AGG TAA GA	20	6182.1
	21-mer i	GCC TGA ACA CCA TAT CCA TCC	21	6292.1
	21-mer ii	ACC GTA AGT AGC ATC ACC TTC	21	6347.1
	21-mer iii	GAC TGG TTC CAA TTG ACA AGC	21	6427.1
	21-mer iv	CGT TCG ACC CCG CCT CGA TCC	21	6276.1
	22-mer i	CTT TTC GGT TAG AGC GGA TGT G	22	6809.1
	22-mer ii	TAC GGT TAC CTT GTT ACG ACT T	22	6688.1
	22-mer iii	TGG TCT TGT TAG AAT TTG TTA C	22	6758.1
	22-mer iv	TCC GGA TTA TTC ATA CCG TCC C	22	6618.1
20-mer OGN and associated manufacturing impurities	FLP	CTC AAA TAT ACT TAC GAT TA	20	6056.1
	N-1	TCA AAT ATA CTT ACG ATT A	19	5767.0
	N-2	CAA ATA TAC TTA CGA TTA	18	5463.0
	N-3	AAA TAT ACT TAC GAT TA	17	5173.9
	N+1	CTC AAA TAT ACT TTA CGA TTA	21	6360.1
Thioated 20-mer OGN and associated manufacturing impurities	FLP	C*T*C* A*A*A* T*A*T* A*C*T* T*A*C* G*A*T* T*A	20	6359.6
	N-1	T*C*A* A*A*T* A*T*A* C*T*T* A*C*G* A*T*T* A	19	6054.6
	N-2	C*A*A* A*T*A* T*A*C* T*T*A* C*G*A* T*T*A	18	5734.6
	N-3	A*A*A* T*A*T* A*C*T* T*A*C* G*A*T* T*A	17	5429.6
	P=O	CT*C* A*A*A* T*A*T* A*C*T* T*A*C* G*A*T* T*A	20	6343.6
	N-1 P=O	T*C*A* A*A*T* A*T*A* C*T*T* A*C*G* A*T*T A	19	6038.6

Gradient 1: Mobile phase A and B. Linear gradient: 20–35% B in 1 min; 35–70% B in 14.1 min; 70–100% B in 3 min. Flow rate: 0.2 ml min^{-1}.

Gradient 2: Mobile phase C and D. Linear gradient: 22.5–25% B in 1 min; 25–90% B in 14.1 min; 70–100% B in 3 min. Flow rate: 0.2 ml min^{-1}.

Gradient 3: Mobile phase E and F. Linear gradient: 20–35% B in 1 min; 35–50% B in 14.1 min; 50–100% B in 3 min. Flow rate: 0.2 ml min^{-1}.

Gradient 4: Mobile phase G and H. Linear gradient: 20–40% B in 7.7 min; 40–80% B in 3.4 min. Flow rate: 0.8 ml min^{-1}.

Gradient 5: Mobile phase C and D. Linear gradient: 27.5–35% B in 1

min; 35–70% B in 14.1 min; 70–100% B in 3 min. Flow rate: 0.2 ml min^{-1}.

Gradient 6: Mobile phase C and D. Linear gradient: 20–35% B in 0.5 min; 35–70% B in 7.05 min; 70–100% B in 1.5 min. Flow rate: 0.2 ml min^{-1}.

2.4. LC-MS analysis

IP-RP (TBuAA) HPLC used for LC-MS analysis on HPLC configuration 1. OGNs were separated using gradient 6 at 30 °C. The HPLC was connected to the mass spectrometer via viper (0.1 mm ID) MP35N tubing into the electrospray ionisation (ESI) source. MS analysis was performed on a Bruker Daltronics MaXis Q-TOF MS in negative mode. The instrument settings were; capillary voltage of 3500 V with endplate offset of 500 V. Ionisation at 350 °C, nebuliser pressure at 35 psi and dry gas delivered at 10 l min^{-1}. Data was acquired over 15 min and analysed using Bruker Compass software (version 1.3, Bruker Daltonics).

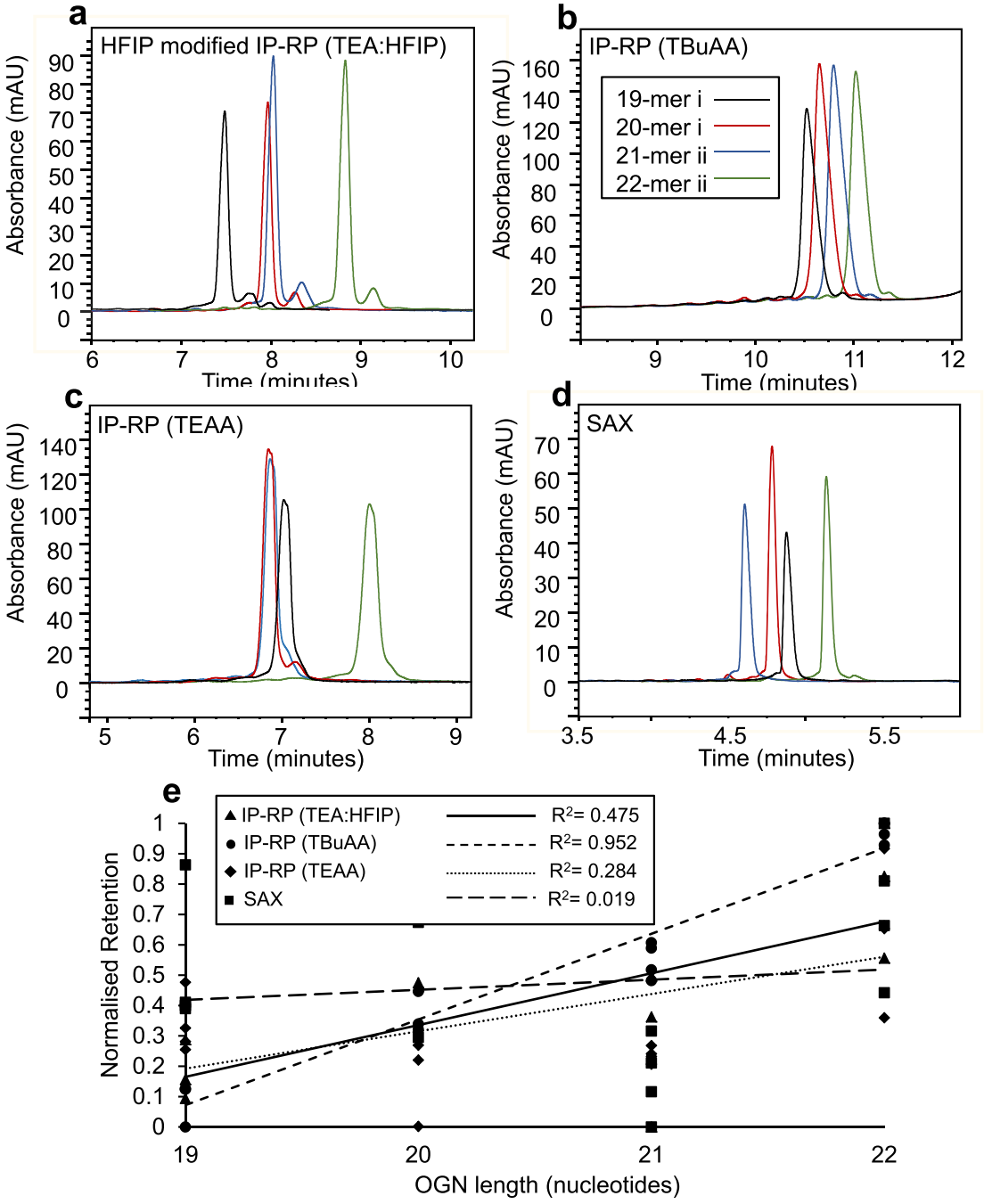

Fig. 1. 19–22-mer size and sequence OGN variant analysis using IP-RP (TEAA/ TEAA:HFIP/ TBuAA) and SAX HPLC to evaluate size and sequence dominant separations. a: HFIP modified IP-RP (TEAA:HFIP) analysis of 30 picomole samples (overlaid) using gradient 1 (methods) at 70 °C. **b:** IP-RP (TBuAA) analysis of 50 picomole samples (overlaid) using gradient 2 at 60 °C. **c:** IP-RP (TEAA) analysis of 50 picomole samples (overlaid) using gradient 3 at 30 °C. **d:** SAX analysis of 30 picomole samples (overlaid) using gradient 4 at 30 °C. OGN legend shown inset in b. **e:** Linear regression analysis between OGN length (nucleotides) and normalised retention value. The coefficient of determination (R^2) is shown for each HPLC condition demonstrating correlation between size and retention. 19–22-mer size and sequence variant OGNs were analysed using the four HPLC conditions (IP-RP using TEAA/ TEAA:HFIP/ TBuAA or SAX) outlined in Fig. 1 a-d. Normalised retention values for all OGNs are shown in Supplementary Table 1.

2.5. Calculations

Analyte retention times were normalised using *Equation (1)* [53], to negate void separation space and normalise retention across different chromatographic gradients. These values were used for calculation of correlation between OGN length (nucleotides) and retention. 2D-LC orthogonality was calculated by plotting normalised retention values against each other in a 2D scatter plot and analysing the minimum convex hull area of the separation space [52]. The minimum convex hull area was calculated using a shoelace algorithm in Python 2.7, followed by conversion to percentage area.

$$Rti(norm) = \frac{Rti - Rt\ \ min}{Rt\ \ max - Rt\ \ min} \quad (1)$$

where *Rt max* and *Rt min* represent the last and first retention times of analytes and *Rti (norm)* values result in integers between 0 and 1.

Peak capacity (n_c) per dimension was calculated using *Equation (2)*. Where T_g is the time of the elution gradient and W is average peak width. Multidimensional theoretical peak capacity was calculated by multiplying dimensional peak capacities: (n_{c*} n_c) = Total peak capacity (n_T).

$$Peak\ \ capacity = \frac{Tg}{W} \quad (2)$$

3. Results and discussion

3.1. 1D-LC analysis of oligonucleotides using IP-RP and SAX HPLC

Initial work focussed on the optimization of size and sequence dependent OGN separations using a range of 1D-LC methods prior to the coupling of these orthogonal modes of chromatography within a 2D-LC workflow. OGNs varying in size and sequence were analysed in four different chromatographic conditions to evaluate retention behaviour. 19–22-mer size and sequence variants (see Table 1) were analysed using IP-RP using a range of conditions including tributylammonium acetate (TBuAA), triethylammonium acetate (TEAA), hexafluoroisopropanol modified IPRP (TEAA:HFIP) and SAX 1D-LC. Analysis of a small subset of the OGN variants that were analysed is shown in each mode in Fig. 1a-d to demonstrate changes in selectivity between the four chromatographic conditions. The retention times of all size and sequence variant OGNs within each 1D-LC analysis were normalised using *Equation (1)* (see Supplementary Table 1) and normalised retention values were plotted against OGN size (in nucleotides) to assess correlation between retention and size (see Fig. 1e). A high correlation (expressed using the coefficient of determination or R^2 value) between retention and OGN size indicates the presence of size dominant separation mechanisms. A low correlation between OGN size and retention indicates OGN base sequence dominant separation mechanisms. The results of Fig. 1e show that the most size dependent separation for these OGNs occurs when using IP-RP in conjunction with TBuAA with an associated R^2 value of 0.952. This observation is consistent with previous studies that demonstrated strongly size dependent separation mechanisms when IP-RP is used in conjunction with hydrophobic ion-pair reagents [27]. Strong IP-RP HPLC using TBuAA is typically employed for the analysis of phosphorothioated OGNs and chemically modified OGN therapeutics due to its predominant size based separation mechanism. Hydrophobic IPRs with long/branched alkyl chains (otherwise known as strong IPRs), such as TBuAA, saturate the stationary phase to a higher degree than an IPR with a lower hydrophobicity (such as TEAA); due to stronger adsorption of the more hydrophobic IPR towards the stationary phase. Increased saturation prevents the occurrence of secondary interactions between the OGN nucleobases and the stationary phase. IP-RP in conjunction with the weaker IP reagent TEAA demonstrates increased sequence based separation mechanisms in comparison with TBuAA (see Fig. 1). It is important to state that broad peak widths are observed for chemically modified OGN therapeutics using TEAA alone.

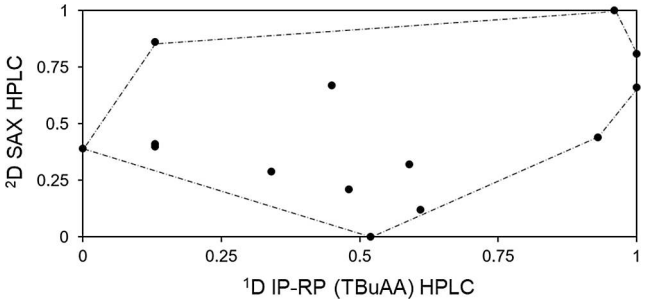

Fig. 2. Orthogonality analysis of 2D HPLC workflows. Minimum convex hull area of 2D separation space for (IP-RP-TBuAA)-(SAX) 2D-LC workflow. Normalised retention values for 19–22-mer size and sequence variant OGNs were plotted with ^{1}D in the x-axis and ^{2}D on the y axis. IP-RP (TbuAA) was used to analyse 50 picomole samples using gradient 2 at 60 °C (x-axis). SAX was used to analyse 30 picomole samples using gradient 4 at 30 °C (y-axis). Normalised retention values for all OGNs shown in Supplementary Table 1.

The results from Fig. 1 show that addition of 40 mM HFIP to the IP-RP (in conjunction with TEAA) mobile phase reduces OGN sequence dependent separations and increases the R^2 value from 0.284 (using TEAA alone) to 0.475. Appfel *et al.,* hypothesized that modifying the mobile phase with an acidic alcohol, such as HFIP, facilitated increased IPR saturation on the stationary phase [36]. The addition of HFIP as a counter ion to the alkylamine in IP-RP HPLC has been widely employed for OGN LC-MS separations [28,51,54,55]. It is important to note that the conditions stated within this work employ HFIP to affect TEAA partitioning and do not use HFIP as the counter ion in lieu of the acetate counter ion. The use of HFIP within this work is to increase the layer of IPR on the stationary phase. The results also show that the selectivity and resolution of closely eluting OGNs is altered when HFIP is added to the mobile phase. This can be seen by comparing resolution of 19-mer i and 20-mer i OGNs (see Fig. 1a/c). In addition, longmers formed during synthesis of the OGNs are also further resolved when 40 mM HFIP is added to the mobile phase (see Fig. 1a). SAX conditions demonstrated the lowest correlation between retention and OGN size with an R^2 value of 0.019. SAX chromatography is known to be a sequence dominant chromatographic mode for the analysis of OGNs- consistent with this data. Increased mobile phase pH (pH 11.5) further ionises tautomeric guanine and thymine OGN nucleobases to allow stronger nucleobase interactions with the stationary phase [20], which increases the dependency on base sequence for separation.

3.1.1. Analysis of phosphorothioate oligonucleotides

Further work was performed to optimise 1D LC separations for the analysis of phosphorothioate OGNs and their associated manufacturing impurities (see Table 1). An additional challenge is presented to develop orthogonal 2D LC workflows for the analysis of phosphorothioate OGNs in that sequence based separations result in low resolution separations due to the large number of diastereoisomers present in phosphorothioate OGNs. Phosphorothioate OGNs could not be eluted from the SAX column using NaCl (data not shown) therefore optimisation was performed using $NaClO_4$ at high pH as our SAX sequence based conditions for both phosphorothioate and unmodified OGNs (avoiding the highly corrosive effects of using NaBr on the LC system). The results are shown in Fig. 3 and demonstrate that peak width increased and selectivity decreased when analysing phosphorothioate OGNs using SAX HPLC. In addition, HFIP modified IP-RP HPLC conditions facilitated improved sequence based separations due to the decrease in peak width from that observed in SAX. This observation demonstrates that the OGN chemistry affects the separation dramatically in different modes of HPLC, furthermore, all conditions apart from TEAA IP-RP HPLC are suitable for OGN therapeutics with higher levels of chemical modification.

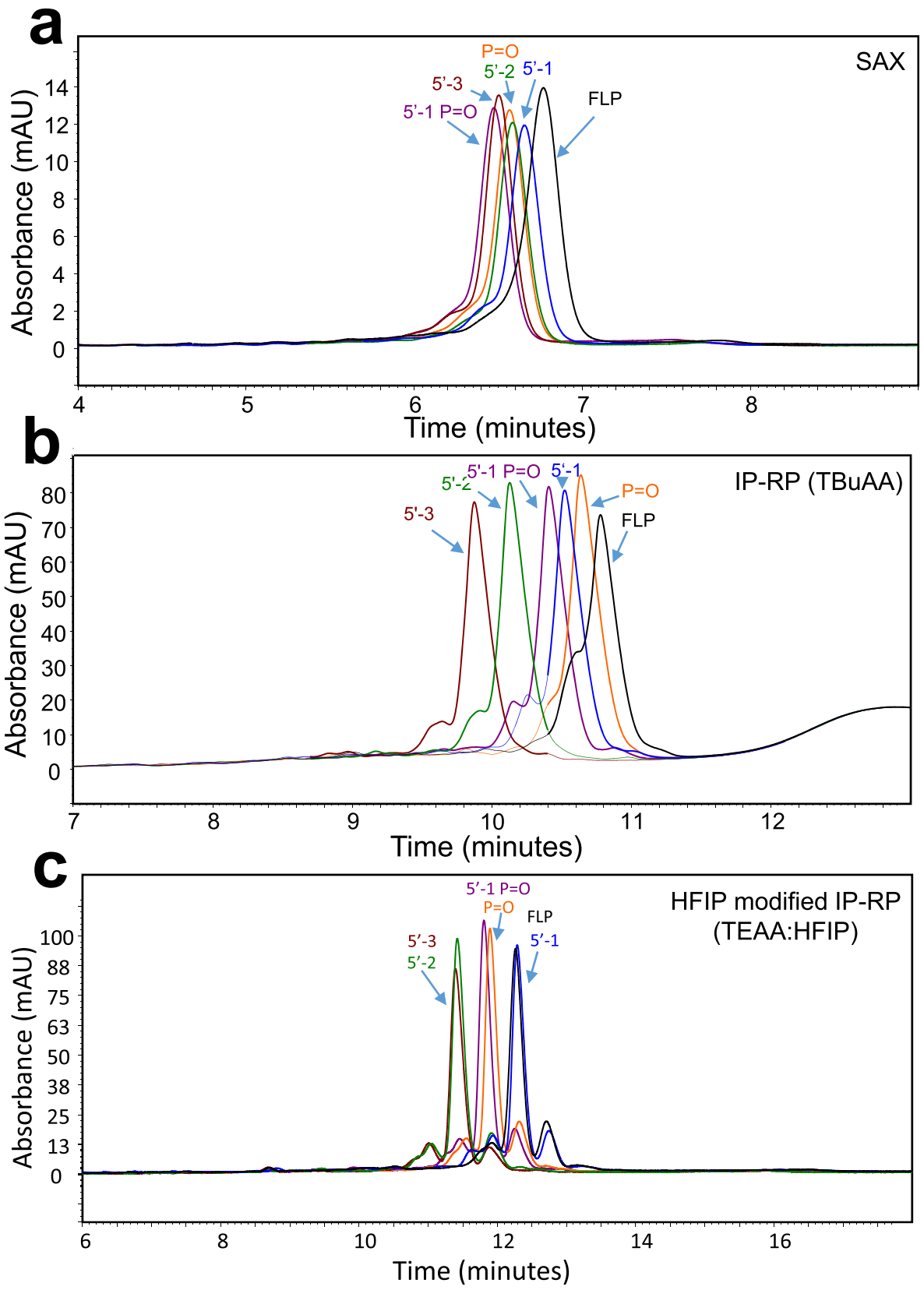

Fig. 3. Separation of a phosphorothioated OGN and associated impurities using SAX, strong IP-RP and HFIP modified IP-RP HPLC conditions. a: SAX HPLC using gradient 4, 30 picomole samples (overlaid) analysed at 30 °C. **b:** Strong IP-RP HPLC using gradient 2, 50 picomole samples (overlaid) analysed at 50 °C. **c:** HFIP modified IP-RP HPLC using gradient 1, 30 picomole samples (overlaid) analysed at 75 °C.

3.2. Orthogonality of 2D-LC workflows

The aim of developing a 2D-LC analytical method is to capitalise on orthogonal separation mechanisms that increase peak capacity by reducing co-elution and increasing resolution. For this work, the basis of orthogonality depends on separation mechanisms that are dominated either by OGN size or OGN base sequence and composition. A 2D-LC workflow that separates by size in one dimension and sequence in another would increase peak capacity by utilising orthogonal dimensional selectivities. Although aimed at comprehensive 2D-LC methods, metrics can also be used as a measure of orthogonality for heart-cut approaches. A simple metric outlined by Rutan *et al.,* is the minimum convex hull method [52]. Normalised retention values of each separation dimension are plotted against each other in a 2D separation space and the area enclosed by outlying values is calculated. This gives an indication of the area of separation space occupied by analytes.

The orthogonality of four alternative theoretical 2D-LC workflows was analysed using the minimum convex hull method. (IP-RP-TBuAA)-(SAX), (IP-RP-TBuAA)-(IP-RP-TEAA), (IP-RP-TBuAA)-(IP-RP-TEAA:HFIP) and (SAX)-(IP-RP-TEAA:HFIP) 2D-LC minimum convex hull orthogonality values are shown in Supplementary Table 2. The results show that the most orthogonal workflow was (IP-RP-TBuAA)-(SAX) 2D-LC with orthogonality value of 66%. These results are consistent with previous analysis of OGNs using 1D LC and demonstrate, as expected, that coupling of a HPLC mode that is the most size dominant separation (IP-RP-TBuAA) with the mode that has the highest sequence based separation (SAX) would result in highest orthogonality value. The least orthogonal 2D-LC workflow was (IP-RP-TBuAA)-(IP-RP-TEAA:HFIP) with an orthogonality value of 38%. The minimum convex hull plot for (IP-RP-TBuAA)-(SAX) 2D-LC is shown in Fig. 2 (see Supplementary Fig. 1 for minimum convex hull plots for (IP-RP-TBuAA)-(IP-RP-TEAA), (IP-RP-TBuAA)-(IP-RP-TEAA:HFIP) and (SAX)-(IP-RP-TEAA:HFIP).

Total peak capacity is an estimate of the maximum number of resolved analytes across the multidimensional separation space. The actual amount of compounds able to be resolved is lower due to separation exclusion zones, random peak placement and peak overlap [46,56-60]. The theoretical total peak capacity of the proposed (IP-RP-TBuAA)-(SAX) 2D-LC method increased by 2 magnitudes in comparison with the peak capacities of either IP-RP using TBuAA 1D-LC or SAX 1D-LC alone. To avoid challenges of peak overlap and low resolution, the most orthogonal workflow was chosen for further method development.

3.3. 2D-LC analysis of oligonucleotides

The HPLC equipment was set up for a multiple heart-cut 2D-LC flow path (see Fig. 4). The 2D-LC flow is enabled by the addition of multi-switch 6 port valves (MSV) in the flow path. The sample is introduced to the 1st dimension analysis via a sampling needle (attached to a fractionation valve) and bridge to the sample loop (attached to a 6 port injection valve). The injection valve (IV) injects the sample onto the 1st dimension column using 1st dimension mobile phase flow from one of two ternary pumps. Upon leaving the UV detector, the fractionation valve (FV) switches position to direct effluent back through the sampling needle into empty micro vials within the autosampler. The MSVs switch position to allow 2nd dimension mobile phase (from a second ternary pump) to flow through the 2nd dimension column re-analyse fractions in a 2nd dimension separation.

Initially, 2nd dimension retention was feasibility tested in an offline method to test compatibility between the eluting conditions of the 1st dimension and the starting conditions of the 2nd dimension. OGNs eluted in approximately 42.5% MeCN in the 1st dimension and were retained in the 2nd dimension. Further development of the method required the optimisation of a UV based detection method for OGNs within the sample set. Aiming to develop a reference mapping strategy, reference oligonucleotides were analysed concurrently to the size and sequence variant OGNs in the 2nd dimension. Reference OGNs were prepared in a diluent matching the eluting conditions of the 1st dimension analysis to avoid retention time shifts due to differences in diluent/eluent between references and samples in the separation. The reference mapping approach was confirmed with comparative MS analysis of the 1st dimension fractions, which were analysed by LC-MS using IP-RP in conjunction with TBuAA.

1D-LC analysis of OGNs in test set 1 (highlighted in Table 1) demonstrated co-elution between OGNs in both SAX and IP-RP (TBuAA) conditions, indicating difficulty in the characterisation of these OGNs. The test mixture was analysed using heart-cut (IP-RP-TBuAA)-(SAX) 2D-LC where OGNs were characterised with reference OGNs in the 2nd dimension (see Fig. 5). To overcome challenges of loss of sensitivity due to dilution within the 2D-LC method, the 1st dimension column was overloaded with sample. This approach reduced resolution of OGNs in the 1st dimension but did not affect resolution in the 2nd dimension of the 2D-LC method.

The 2D-LC method overcame co-elution of OGNs in the 1st dimension by orthogonal resolution in the 2nd dimension, exemplified by assessment of OGNs 19-mer i and iii in the 1st dimension. The two OGNs from ^{1}D fractions 1 and 2 resolve in the SAX 2nd dimension separation, whereas they co-elute under a single peak in the 1st dimension. 19-mer iii OGN co-elutes with the 22-mer ii OGN using SAX 1D-LC (see Fig. 5), which is avoided by using size based separation in a 1st dimension using IP-RP (TBuAA). Therefore, in the 2D-LC method, 22-mer ii elutes in fractions 4–6 away from 19-mer iii in earlier fractions (1 and 2). The 20-mer i and 21-mer iv OGNs closely elute using IP-RP (TBuAA) 1D-LC conditions. Using a 2D-LC method, these OGNs are further resolved in fractions 2–3 of the 2nd dimension. Further demonstration of improved

Table 2
LC-MS identification of 19–22-mer size and sequence variant OGN masses in each fraction of the 1st dimension analysis. IP-RP in conjunction with TBuAA was used to separate OGNs and extract 6 fractions using gradient 6 at 30 °C. Mass spectrometry OGN identification was performed by identification of 4^{-} charge state ion monoisotopic masses.

Fraction	OGN Observed Monoisotopic Mass (Da)	OGN Theoretical Monoisotopic Mass (Da)	Observed Monoisotopic *m/z* of [M−4H] 4^{-}	Theoretical Monoisotopic *m/z* of [M−4H] 4^{-}	Identity Assignment
1	5807.204	5806.980	1450.793	1450.737	19-mer i
	5930.248	5930.022	1481.554	1481.497	19-mer iii
2	6113.284	6113.054	1527.313	1527.255	20-mer i
	5807.204	5806.980	1450.793	1450.737	19-mer i
	6276.288	6276.056	1568.064	1568.006	21-mer iv
	5930.252	5930.022	1481.555	1481.497	19-mer iii
3	6113.288	6113.054	1527.314	1527.255	20-mer i
	6276.284	6276.056	1568.063	1568.006	21-mer iv
4	6618.372	6618.117	1653.585	1653.521	22-mer iv
	6688.360	6688.123	1671.082	1671.023	22-mer ii
5	6688.372	6688.123	1671.085	1671.023	22-mer ii
	6618.372	6618.117	1653.585	1653.521	22-mer iv
6	6688.368	6688.123	1671.084	1671.023	22-mer ii

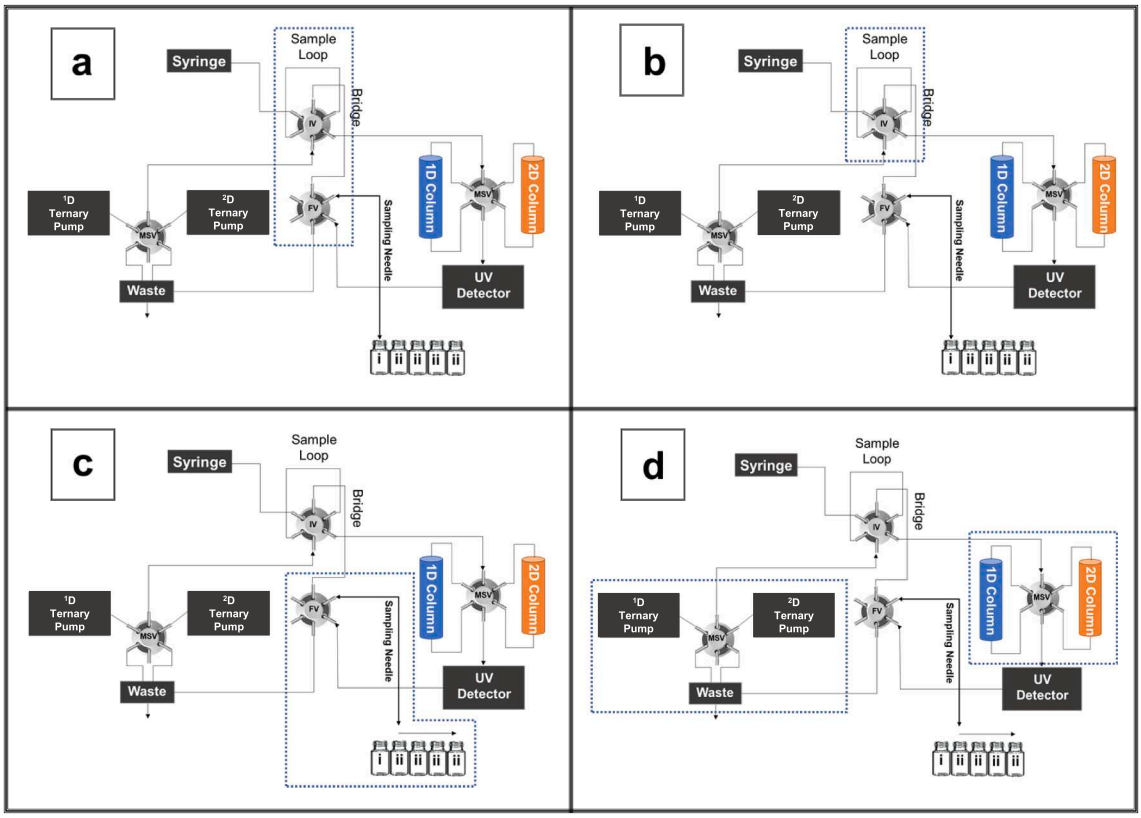

Fig. 4. 2D-LC configuration. a: ^{1}D sample (i) is introduced via a sampling needle and bridge to the sample loop (boxed area). **b:** The injection valve (IV) (boxed area) injects the sample onto the 1st dimension column using 1st dimension mobile phase. **c:** Upon leaving the UV detector, the fractionation valve (FV) switches position (boxed area) to direct ^{1}D effluent back through the sampling needle into empty micro vials (ii). **d:** The multi-switch valves (MSV) switch position (boxed areas) to allow 2nd dimension mobile phase to flow through the ^{2}D column and the fractions (ii) are re-analysed.

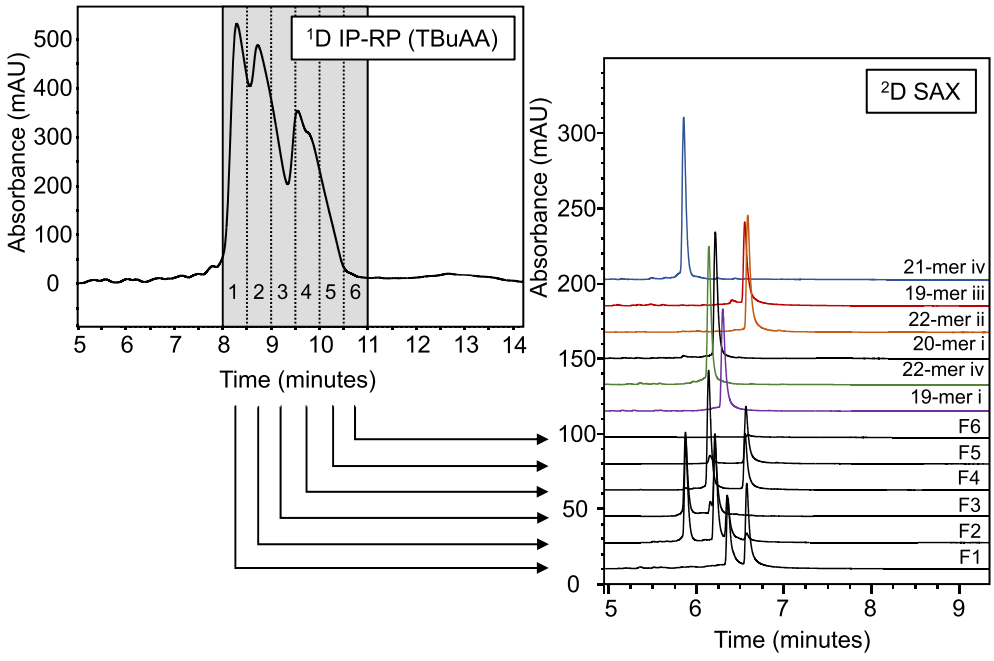

Fig. 5. 2D-LC analysis if 19–22-mer size and sequence OGN. (IP-RP-TBuAA)-(SAX) 2D-LC of 1000 picomole mixed OGN sample using gradient 5 at 50 °C (^{1}D) and Gradient 4 at ambient temperature (^{2}D) alongside reference OGNs at 30 picomole sample amount..

characterisation of OGNs in a second test set using of orthogonal separations within the 2D-LC method is shown in Supplementary Fig. 2. LC-MS analysis was also performed to confirm the ability of reference mapping strategy to identify OGNs within the mixture (see Table 2 and Supplementary Table 3). The LC-MS results complement the reference mapping data. Optimisation of the UV based reference mapping strategy

reduces the requirement for complex detection methods, such as routine use of MS. The key benefits of this are a reduction in analytical complexity, equipment usage and the ability to implement the method into manufacturing processes with reduced requirements on technical expertise.

The 2D-LC method was also performed using a 20-mer OGN mixed with its associated OGN manufacturing impurities added at 1.5% concentration (see Fig. 6). In the 1st dimension, a number of the OGN manufacturing impurities at low concentration typically co-elute under or closely elute near the main peak of the full-length product OGN, which would affect characterisation of these impurities using 1D-LC with UV analysis alone. The results show that using the 2D-LC method, the shortmer and longmer impurities were identified using the reference mapping strategy. Utilisation of an orthogonal 2D-LC method also enabled the separation of other impurities, including impurities that would otherwise co-elute with the full length oligonucleotide product (FLP) in 1D-LC conditions. This was demonstrated in Fig. 6 where an impurity co-eluting under the FLP peak in Fraction 3 of the IP-RP ^{1}D is prevented from co-eluting with the N + 1 peak at 5.9 min Rt in the ^{2}D SAX separation (highlighted with a red asterix). Separation of analytes that would co-elute in SAX HPLC using this 2D-LC workflow increased the accuracy of characterisation of the N + 1 impurity; identified in Fractions 6 and 7. Reduction in co-elution events was enabled by using an orthogonal size dependent separation in the 1st dimension, followed by a sequence dependent separation in the 2nd dimension.

A high amount of acetonitrile was required to elute phosphorothioate OGNs from the 1st dimension IP-RP TBuAA column, which impeded retention in the 2nd dimension SAX HPLC separation (data not shown). Therefore alternative 2D-LC workflows using (SAX)-(IP-RP-TBuAA) or (IP-RP-TEAA/HFIP)-(SAX) are potential alternative approaches.

4. Conclusions

In this study we optimized size and sequence based OGN separations using a variety of 1D-LC methods and coupled orthogonal modes of chromatography within a 2D-LC workflow. A heart-cut (IP-RP-TBuAA)-(SAX-$NaClO_4$) 2D-LC method in conjunction with UV detection was developed to overcome challenges of co-elution and low selectivity of OGN size and sequence variants and improve the characterisation of OGN manufacturing impurities (shortmer and longmer failed sequences). The results show that the (IP-RP- SAX) 2D-LC method reduced co-elution and increased selectivity of closely-related OGNs. This approach also facilitated improved separation of unmodified synthetic OGNs and their respective OGN impurities. The benefit of adopting this 2D-LC approach is that the application of a UV based reference mapping strategy using reference OGNs enabled the reduction of analytical complexity by reducing the reliance on mass based detection methods. The development of 2D-LC methods that do not rely upon MS based detection have a number of potential advantages including; reduction in analytical complexity, reducing the use of expensive instrumentation, enabling increased throughput with simple operation/data analysis and an increase in the ease of operation for manufacturing staff. This 2D-LC chromatographic method was developed using a self-designed system, highlighting reduced requirement for specialist, expensive 2D-LC equipment and is a demonstration of the application of multidimensional chromatography using HPLC equipment more commonly found within the laboratory. As this approach is based upon qualitative detection, the 2D-LC method is best placed in a chemical or manufacturing development environment to aid in the optimisation of synthesis or process design enabling LC based OGN impurity tracking. The orthogonality of the method is estimated to remain high for unmodified OGNs and OGNs with low levels of chemical modification. The 2D-LC method developed in this study also has further potential applications where complex mixtures of OGNs require analysis, for example,

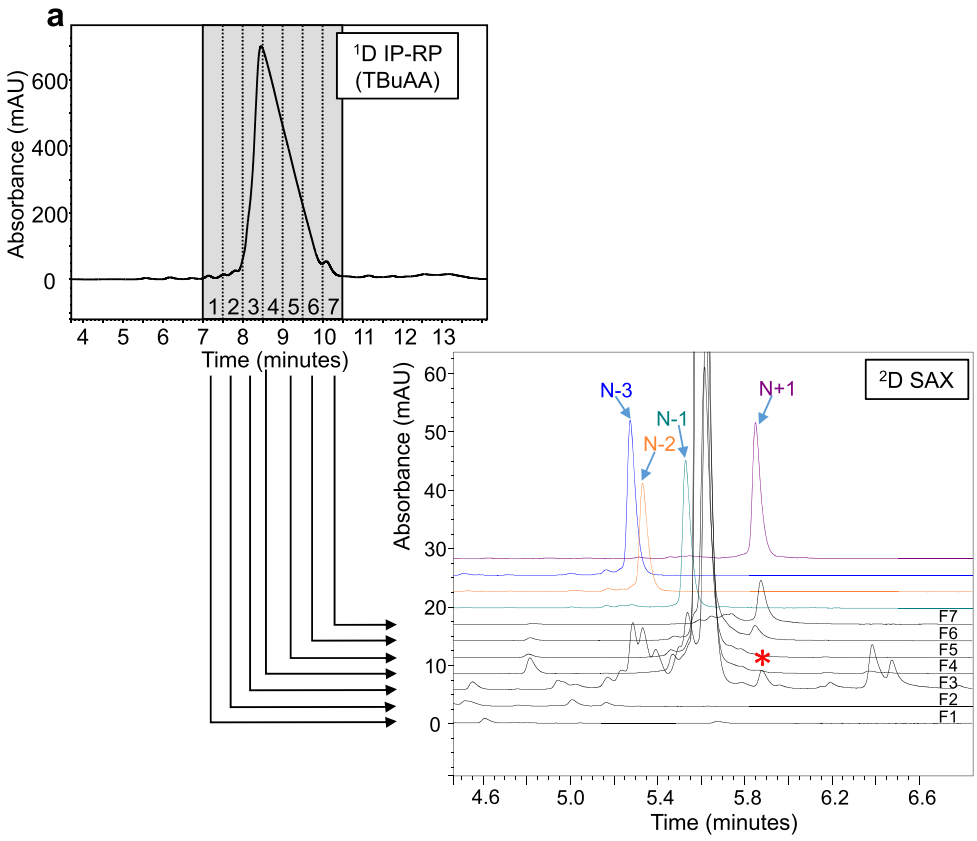

Fig. 6. 2D-LC analysis of OGN and associated manufacturing impurities. a: (IP-RP-TBuAA)-(SAX) 2D-LC of 1000 picomole spiked OGN sample with 1.5% added concentration OGN impurities using gradient 5 at 50 °C (^{1}D) and Gradient 4 at ambient temperature (^{2}D) alongside reference OGNs at 10 picomole sample amount. Red asterix above peak in Fraction 3 indicates co-eluting impurity. (For interpretation of the references to colour in this figure legend, the reader is referred to the web version of this article.)

within RNase mapping or resolution of oligonucleotides with single nucleotide polymorphisms. Furthermore, the 2D-LC method could also be utilised symbiotically with 1D-LC-MS approaches to confirm or align with quantitative 1D-LC data.

CRediT authorship contribution statement

Christina Vanhinsbergh: Conceptualization, Methodology, Validation, Investigation, Formal analysis, Data curation, Visualization, Writing – original draft. **Elliot C. Hook:** Conceptualization, Supervision, Writing – review & editing, Funding acquisition. **Nicola Oxby:** Conceptualization, Supervision, Writing – review & editing, Funding acquisition. **Mark J. Dickman:** Conceptualization, Supervision, Writing – original draft, Writing – review & editing, Project administration, Funding acquisition.

Declaration of Competing Interest

The authors declare that they have no known competing financial interests or personal relationships that could have appeared to influence the work reported in this paper.

Data availability

Data will be made available on request.

Acknowledgements

This work was supported by Biotechnology and Biological Sciences Research Council Training Grant/GSK [BB/K501086/1]. In addition, MJD acknowledges support from the Biotechnology and Biological Sciences Research Council [BB/M012166/1].

Appendix A. Supplementary data

Supplementary data to this article can be found online at https://doi.org/10.1016/j.jchromb.2023.123812.

References

[1] A. Khvorova, J.K. Watts, The chemical evolution of oligonucleotide therapies of clinical utility, Nat. Biotechnol. (2017), https://doi.org/10.1038/nbt.3765.
[2] S.M. Nimjee, R.R. White, R.C. Becker, B.A. Sullenger, Aptamers as Therapeutics, in: Annu. Rev. Pharmacol. Toxicol. vol. 57, ed, 2017, pp. 61-79.
[3] C.A. Stein, D. Castanotto, FDA- Approved Oligonucleotide Therapies in 2017, Mol. Ther. 25 (5) (2017) 1069–1075, https://doi.org/10.1016/j.ymthe.2017.03.023.
[4] S.-N. Park, Y. Lim, J.-K. Kook, Development of quantitative real-time PCR primers for detecting 42 oral bacterial species, Arch. Microbiol. 195 (7) (2013) 473–482, https://doi.org/10.1007/s00203-013-0896-4.
[5] R.J. Fernandes, S.S. Skiena, Microarray synthesis through multiple- use PCR primer design, Bioinformatics 18 (1) (2002) 128–135.
[6] L. Cong et al., Multiplex genome engineering using CRISPR/Cas systems, Science (New York, N.Y.) 339(6121) (2013) 819-823, 10.1126/science.1231143.
[7] A.C. McGinnis, B. Chen, M.G. Bartlett, Chromatographic methods for the determination of therapeutic oligonucleotides, J. Chromatogr. B 883–884 (2012) 76–94, https://doi.org/10.1016/j.jchromb.2011.09.007.
[8] I.C. Santos, J.S. Brodbelt, Recent developments in the characterization of nucleic acids by liquid chromatography, capillary electrophoresis, ion mobility, and mass spectrometry (2010–2020), J. Sep. Sci. 44 (1) (2021) 340–372, https://doi.org/10.1002/jssc.202000833.
[9] S. Roy, M. Caruthers, Synthesis of DNA/ RNA and Their Analogs via Phosphoramidite and H- Phosphonate Chemistries, in: Molecules vol. 18, ed, 2013, pp. 14268-14284.
[10] A.H. Krotz, P.G. Klopchin, K.L. Walker, G.S. Srivatsa, D.L. Cole, V.T. Ravikumar, On the formation of longmers in phosphorothioate oligodeoxyribonucleotide synthesis, Tetrahedron Lett. 38 (22) (1997) 3875–3878, https://doi.org/10.1016/S0040-4039(97)00798-3.
[11] K.L. Fearon, J.T. Stults, B.J. Bergot, L.M. Christensen, A.M. Raible, Investigation of the ' n- 1' impurity in phosphorothioate oligodeoxynucleotides synthesized by the solid- phase beta- cyanoethyl phosphoramidite method using stepwise sulfurization, Nucleic Acids Res. 23 (14) (1995) 2754.
[12] J. Temsamani, M. Kubert, S. Agrawal, Sequence identity of the n- 1 product of a synthetic oligonucleotide, Nucleic Acids Res. 23 (11) (1995) 1841.
[13] N. Elzahar, N. Magdy, A. El-Kosasy, M. Bartlett, Degradation product characterization of therapeutic oligonucleotides using liquid chromatography mass spectrometry, Anal. Bioanal. Chem. 410 (14) (2018) 3375–3384, https://doi.org/10.1007/s00216-018-1032-8.
[14] D. Capaldi, et al., Impurities in Oligonucleotide Drug Substances and Drug Products, Nucleic Acid Ther. 27 (6) (2017) 39–322, https://doi.org/10.1089/nat.2017.0691.
[15] D. Capaldi, et al., Quality Aspects of Oligonucleotide Drug Development: Specifications for Active Pharmaceutical Ingredients, Ther. Innov. Regul. Sci. 46 (5) (2012) 611–626, https://doi.org/10.1177/0092861512445311.
[16] A.C. McGinnis, B.S. Cummings, M.G. Bartlett, Ion exchange liquid chromatography method for the direct determination of small ribonucleic acids, Anal. Chim. Acta 799 (2013) 57–67, https://doi.org/10.1016/j.aca.2013.08.040.
[17] S.G. Roussis, M. Pearce, C. Rentel, Small alkyl amines as ion-pair reagents for the separation of positional isomers of impurities in phosphate diester oligonucleotides, J. Chromatogr. A 1594 (2019) 105–111, https://doi.org/10.1016/j.chroma.2019.02.026.
[18] E. Largy, J.-L. Mergny, Shape matters: size- exclusion HPLC for the study of nucleic acid structural polymorphism, Nucleic Acids Res. 42 (19) (2014) e149.
[19] P.A. Lobue, M. Jora, B. Addepalli, P.A. Limbach, Oligonucleotide analysis by hydrophilic interaction liquid chromatography-mass spectrometry in the absence of ion-pair reagents, J. Chromatogr. A 1595 (2019) 39–48, https://doi.org/10.1016/j.chroma.2019.02.016.
[20] J.R. Thayer, V. Barreto, S. Rao, C. Pohl, Control of oligonucleotide retention on a pH- stabilized strong anion exchange column, Anal. Biochem. 338 (1) (2005) 39–47, https://doi.org/10.1016/j.ab.2004.11.013.
[21] M. Bunček, et al., Retention Behavior of Oligonucleotides on a Glycidyl Methacrylate- Based DEAE-Modified Sorbent, Chroma 62 (5) (2005) 263–269, https://doi.org/10.1365/s10337-005-0620-x.
[22] M. Bunček, et al., Unusual chromatographic behavior of oligonucleotide sequence isomers on two different anion exchange HPLC columns, Anal. Biochem. 348 (2) (2006) 300–306, https://doi.org/10.1016/j.ab.2005.10.047.
[23] S. Yamamoto, M. Nakamura, C. Tarmann, A. Jungbauer, Retention studies of DNA on anion- exchange monolith chromatography: Binding site and elution behavior, J. Chromatogr. A 1144 (1) (2007) 155–160, https://doi.org/10.1016/j.chroma.2007.01.025.
[24] P.J. Oefner, Allelic discrimination by denaturing high- performance liquid chromatography, J. Chromatogr. B Biomed. Sci. Appl. 739 (2) (2000) 345–355, https://doi.org/10.1016/S0378-4347(99)00571-X.
[25] M. Gilar, Analysis and Purification of Synthetic Oligonucleotides by Reversed-Phase High-Performance Liquid Chromatography with Photodiode Array and Mass Spectrometry Detection, Anal. Biochem. 298 (2) (2001) 196–206, https://doi.org/10.1006/abio.2001.5386.
[26] A. Azarani, K.H. Hecker, RNA analysis by ion- pair reversed- phase high performance liquid chromatography, Nucleic Acids Res. 29 (2) (2001) E7.
[27] A. McKeown, P. Shaw, D. Barrett, Retention behaviour of an homologous series of oligodeoxythymidilic acids using reversed-phase ion-pair chromatography, Chromatographia 55 (5) (2002) 271–277, https://doi.org/10.1007/BF02491658.
[28] M. Gilar, et al., Ion-pair reversed-phase high-performance liquid chromatography analysis of oligonucleotides: Retention prediction, J. Chromatogr. A 958 (1) (2002) 167–182, https://doi.org/10.1016/S0021-9673(02)00306-0.
[29] M.J. Dickman, M.J. Conroy, J.A. Grasby, D.P. Hornby, RNA footprinting analysis using ion pair reverse phase liquid chromatography, RNA 8 (2) (2002) 247–251.
[30] M.J. Dickman, Effects of sequence and structure in the separation of nucleic acids using ion pair reverse phase liquid chromatography, J. Chromatogr. A 1076 (1) (2005) 83–89, https://doi.org/10.1016/j.chroma.2005.04.018.
[31] M.J. Dickman, D.P. Hornby, Enrichment and analysis of RNA centered on ion pair reverse phase methodology, RNA 12 (4) (2006) 691–696, https://doi.org/10.1261/rna.2278606.
[32] S.P. Waghmare, P. Pousinis, D.P. Hornby, M.J. Dickman, Studying the mechanism of RNA separations using RNA chromatography and its application in the analysis of ribosomal RNA and RNA:RNA interactions, J. Chromatogr. A 1216 (9) (2009) 1377–1382, https://doi.org/10.1016/j.chroma.2008.12.077.
[33] E.D. Close, et al., Nucleic acid separations using superficially porous silica particles, J. Chromatogr. A 1440 (2016) 135–144, https://doi.org/10.1016/j.chroma.2016.02.057.
[34] L. Gong, Comparing ion-pairing reagents and counter anions for ion-pair reversed-phase liquid chromatography/electrospray ionization mass spectrometry analysis of synthetic oligonucleotides, Rapid Commun. Mass Spectrom. 29 (24) (2015) 2402–2410, https://doi.org/10.1002/rcm.7409.
[35] B. Basiri, H. Hattum, W. Dongen, M. Murph, M. Bartlett, The Role of Fluorinated Alcohols as Mobile Phase Modifiers for LC-MS Analysis of Oligonucleotides, Off. J. Am. Soc. Mass Spectrometry 28 (1) (2017) 190–199, https://doi.org/10.1007/s13361-016-1500-3.
[36] A. Apffel, J.A. Chakel, S. Fischer, K. Lichtenwalter, W.S. Hancock, New procedure for the use of high-performance liquid chromatography–electrospray ionization mass spectrometry for the analysis of nucleotides and oligonucleotides, J. Chromatogr. A 777 (1) (1997) 3–21.
[37] Z. Huang, S. Jayaseelan, J. Hebert, H. Seo, L. Niu, Single- nucleotide resolution of RNAs up to 59 nucleotides by high- performance liquid chromatography, Anal. Biochem. (2012), https://doi.org/10.1016/j.ab.2012.12.011.
[38] S.G. Roussis, A.A. Rodriguez, C. Rentel, Determination of individual oligonucleotide impurities by small amine ion pair-RP HPLC MS and MS/MS: n− 1 impurities, J. Chromatogr. B 1169 (2021), 122611.

[39] W. Brad Wan, P.P. Seth, The Medicinal Chemistry of Therapeutic Oligonucleotides, J. Med. Chem. 59 (21) (2016) 9645–9667, https://doi.org/10.1021/acs.jmedchem.6b00551.
[40] I. Nikcevic, T.K. Wyrzykiewicz, P.A. Limbach, Detecting low- level synthesis impurities in modified phosphorothioate oligonucleotides using liquid chromatography– high resolution mass spectrometry, Int. J. Mass Spectrom. 304 (2–3) (2011) 98–104, https://doi.org/10.1016/j.ijms.2010.06.001.
[41] M. Smith, T. Beck, Quantitation of a low level coeluting impurity present in a modified oligonucleotide by both LC-MS and NMR, J. Pharm. Biomed. Anal. 118 (2016) 34–40, https://doi.org/10.1016/j.jpba.2015.10.019.
[42] C.-L. Yao, et al., Global profiling combined with predicted metabolites screening for discovery of natural compounds: Characterization of ginsenosides in the leaves of Panax notoginseng as a case study, J. Chromatogr. A 1538 (2018) 34–44, https://doi.org/10.1016/j.chroma.2018.01.040.
[43] C. Armutcu, E. Özgür, T. Karasu, E. Bayram, L. Uzun, M. Çorman, Rapid Analysis of Polycyclic Aromatic Hydrocarbons in Water Samples Using an Automated On-line Two-Dimensional Liquid Chromatography, Int. J. Environ. Pollut. 230 (10) (2019) 1–11, https://doi.org/10.1007/s11270-019-4306-7.
[44] H. Zhao, et al., An improved 2D-HPLC-UF-ESI-TOF/MS approach for enrichment and comprehensive characterization of minor neuraminidase inhibitors from Flos Lonicerae Japonicae, J. Pharm. Biomed. Anal. 175 (2019), https://doi.org/10.1016/j.jpba.2019.07.006.
[45] G. Vanhoenacker, I. Vandenheede, F. David, P. Sandra, K. Sandra, Comprehensive two- dimensional liquid chromatography of therapeutic monoclonal antibody digests, Anal. Bioanal. Chem. 407 (1) (2015) 355–366, https://doi.org/10.1007/s00216-014-8299-1.
[46] D.R. Stoll, P.W. Carr, Two-Dimensional Liquid Chromatography: A State of the Art Tutorial, Anal. Chem. 89 (1) (2017) 519–531, https://doi.org/10.1021/acs.analchem.6b03506.
[47] Q. Li, F. Lynen, J. Wang, H. Li, G. Xu, P. Sandra, Comprehensive hydrophilic interaction and ion- pair reversed- phase liquid chromatography for analysis of di- to deca- oligonucleotides, J. Chromatogr. A 1255 (2012) 237–243, https://doi.org/10.1016/j.chroma.2011.11.062.
[48] P. Álvarez Porebski, F. Lynen, Combining liquid chromatography with multiplexed capillary gel electrophoresis for offline comprehensive analysis of complex oligonucleotide samples, J. Chromatogr. A, 1336 (2014) 87-93, 10.1016/j.chroma.2014.02.007.
[49] C. Anacleto, R. Ouye, N. Schoenbrunner, Orthogonal ion pairing reversed phase liquid chromatography purification of oligonucleotides with bulky fluorophores, J. Chromatogr. A 1329 (2014) 78–82, https://doi.org/10.1016/j.chroma.2013.12.072.
[50] S.G. Roussis, I. Cedillo, C. Rentel, Two-dimensional liquid chromatography-mass spectrometry for the characterization of modified oligonucleotide impurities, Anal. Biochem. 556 (2018) 45–52, https://doi.org/10.1016/j.ab.2018.06.019.
[51] A. Goyon, K. Zhang, Characterization of Antisense Oligonucleotide Impurities by Ion-Pairing Reversed-Phase and Anion Exchange Chromatography Coupled to Hydrophilic Interaction Liquid Chromatography/Mass Spectrometry Using a Versatile Two-Dimensional Liquid Chromatography Setup, Anal. Chem. 92 (8) (2020) 5944–5951.
[52] S.C. Rutan, J.M. Davis, P.W. Carr, Fractional coverage metrics based on ecological home range for calculation of the effective peak capacity in comprehensive two-dimensional separations, J. Chromatogr. A 1255 (2012) 267–276, https://doi.org/10.1016/j.chroma.2011.12.061.
[53] M. Gilar, P. Olivova, A.E. Daly, J.C. Gebler, Orthogonality of separation in two-dimensional liquid chromatography, Anal. Chem. 77 (19) (2005) 6426–6434, https://doi.org/10.1021/ac050923i.
[54] G. Dai, X. Wei, Z. Liu, S. Liu, G. Marcucci, K.K. Chan, Characterization and quantification of Bcl-2 antisense G3139 and metabolites in plasma and urine by ion-pair reversed phase HPLC coupled with electrospray ion-trap mass spectrometry, J. Chromatogr. B 825 (2) (2005) 201–213, https://doi.org/10.1016/j.jchromb.2005.05.049.
[55] R. Erb, H. Oberacher, Comparison of mobile-phase systems commonly applied in liquid chromatography-mass spectrometry of nucleic acids, Electrophoresis 35 (9) (2014) 1226–1235, https://doi.org/10.1002/elps.201300269.
[56] M. Gilar, U.D. Neue, Peak capacity in gradient reversed-phase liquid chromatography of biopolymers. Theoretical and practical implications for the separation of oligonucleotides, J. Chromatogr. A 1169 (1–2) (2007) 139–150, https://doi.org/10.1016/j.chroma.2007.09.005.
[57] U.D. Neue, Theory of peak capacity in gradient elution, J. Chromatogr. A 1079 (1–2) (2005) 153–161, https://doi.org/10.1016/j.chroma.2005.03.008.
[58] D.R. Stoll, J.D. Cohen, P.W. Carr, Fast, comprehensive online two-dimensional high performance liquid chromatography through the use of high temperature ultra-fast gradient elution reversed-phase liquid chromatography, J. Chromatogr. A 1122 (1–2) (2006) 123–137, https://doi.org/10.1016/j.chroma.2006.04.058.
[59] K. Horie, et al., Calculating optimal modulation periods to maximize the peak capacity in two-dimensional HPLC, Anal. Chem. 79 (10) (2007) 3764–3770, https://doi.org/10.1021/ac062002t.
[60] D. Li, C. Jakob, O. Schmitz, Practical considerations in comprehensive two-dimensional liquid chromatography systems (LCxLC) with reversed-phases in both dimensions, Anal. Bioanal. Chem. 407 (1) (2015) 153–167, https://doi.org/10.1007/s00216-014-8179-8.